UDC 621.3 https://doi.org/10.20998/2074-272X.2025.3.05

L. Djafer, R. Taleb, F. Mehedi, A. Aissa Bokhtache, T. Bessaad, F. Chabni, H. Saidi

Electric drive vehicle based on sliding mode control technique using a 21-level asymmetrical inverter under different operating conditions

Introduction. *Electric vehicles (EVs) have drawn increased attention as a possible remedy for the energy crisis and environmental issues. These days, EVs can be propelled by an extensive range of power electronics to produce the energy required for the motor and operate efficiently at high voltage levels. Multilevel inverters (MLIs) were designed to address the challenges and limitations of traditional converters .**The novelty** of the research that is being presented a 21-asymmetric MLI with reduced switching using pulse width modulation technique for powering electric propulsion system of EVs, with the proposed topology delivering notable enhancements in both performance and cost-efficiency compared to conventional asymmetric designs. **Purpose.** Improving EV performance by utilizing sliding mode control (SMC) technique for controlling a permanent magnet synchronous motor (PMSM) powered by a 21-level reduced switching inverter topology. **Methods.** This study focuses on assessing the feasibility of a 21-asymmetric MLI with reduced switching. This inverter utilize different input voltage levels for various components and modules, enabling the combination and subtraction of these voltages to create multiple voltage levels for use in the traction system of electric vehicles, designed to power a PMSM. The motor's operation is controlled using SMC technique with three distinct surfaces, with consideration for the vehicle's dynamic behavior. **Results.** Proved that, using a 21-asymmetric MLI to optimize the quality of the output voltage for improving the performance of the EV. The proposed topology offers a cost-effective and simple system that is easy to maintain. **Practical value.** To assess the effectiveness and resilience of the suggested control system, we conducted simulations using MATLAB/Simulink. Notably, the target speed adheres to the urban driving schedule in Europe, specifically the ECE-15 cycle.* References 21, tables 2, figures 10.

Key words: **asymmetric multilevel inverter, electric vehicle, permanent magnet synchronous motor, sliding mode control.**

Вступ. *Електромобілі (EVs) привернули підвищену увагу як можливий засіб від енергетичної кризи та екологічних проблем. У наші дні EVs можуть рухатися широким спектром силової електроніки для вироблення енергії, необхідної для двигуна, і працювати ефективно при високих рівнях напруги. Багаторівневі інвертори (MLI) були розроблені для вирішення проблем та обмежень традиційних перетворювачів. **Новизна** дослідження, яке представлено, 21-асиметричний MLI зі зменшеним перемиканням, що використовує метод широтно-імпульсної модуляції для живлення електричної рухової системи EVs, з запропонованою топологією, що забезпечує помітне покращення як продуктивності, так і економічної ефективності порівняно з традиційними асиметричними конструкціями. **Мета**. Поліпшення продуктивності EVs за рахунок використання методу керування ковзним режимом (SMC) для керування синхронним двигуном з постійними магнітами (PMSM), що працює від топології 21-рівневого інвертора зі зменшеним перемиканням. **Методи**. Це дослідження зосереджено на оцінці здійсненності 21-асиметричного MLI зі зменшеним перемиканням. Цей інвертор використовує різні рівні вхідної напруги для різних компонентів та модулів, що дозволяє комбінувати та віднімати цю напругу для створення кількох рівнів напруги для використання в тяговій системі електромобілів, призначеної для живлення PMSM. Робота двигуна контролюється за допомогою техніки SMC із трьома різними поверхнями з урахуванням динамічної поведінки автомобіля. **Результати**. Доведено, що використання 21-асиметричного MLI для оптимізації якості вихідної напруги покращує продуктивність EV. Запропонована топологія пропонує економічну та просту систему, яку легко обслуговувати. **Практична цінність**. Для оцінки ефективності та стійкості запропонованої системи управління ми здійснили моделювання з використанням MATLAB/Simulink. Зокрема цільова швидкість відповідає міському графіку водіння в Європі, зокрема циклу ECE-15.* Бібл. 21, табл. 2, рис. 10.

Ключові слова: **асиметричний багаторівневий інвертор, електромобіль, синхронний двигун з постійними магнітами, керування ковзним режимом.**

Introduction. The growing challenge of global warming and air emissions from transportation in urban areas has led to the development of various alternative mobility solutions, such as electric vehicles (EV), car sharing, and e-bikes [1]. EV presents multiple benefits: electric energy is more affordable and environmentally friendly compared to oil, electric motors are more efficient than internal combustion engines, EV operate more quietly, and they can be charged at home [2]. Consequently, this remains essential for the research community to prioritize clean, renewable, and environmentally friendly energy sources and to encourage policy and economic leaders to take decisive action to tackle this issue and facilitate the shift to renewable energy. In this situation, the growing presence of EV in a fiercely competitive market drives car manufacturers to create more fuel-efficient automobiles at lower expenses. Key performance criteria for EV encompass reliability, resilience, energy control, battery charging rate, and especially the electric drive system [3].

The fuel cell serves as the primary source of energy in the EV power supply, nevertheless, in low-load situations, the fuel cell may prove inadequate, making it necessary to use a battery as a backup source to prevent a limited range of driving distance and extend the lifespan of the fuel cell [4]. Consequently, energy management is optimized to enable energy distribution among the propulsion system components, along with the appropriate selection of the motor.

A permanent magnet synchronous motor (PMSM) is widely used in EV energy propulsion systems because of its numerous advantages, such as its efficient compact structure, high air-gap flux density, high energy density, favorable torque-to-inertia ratio, and excellent performance effectiveness [5]. PMSM necessitates an effective management strategy, meaning it demands a rapid and precise response, swift recovery from disturbances, and robustness against variations in parameters. As a result, numerous contemporary control techniques, including sliding mode control (SMC), have been advocated to enhance the performance of the PMSM [6].

SMC technique is a popular technique because it effectively rejects internal parameter changes and outside disruptions. SMC has discovered vast application in

© L. Djafer, R. Taleb, F. Mehedi, A. Aissa Bokhtache, T. Bessaad, F. Chabni, H. Saidi

electrical power systems and electrical devices for machines [7, 8]. As a result, it has been effectively utilized for controlling the position and speed of PMSMs.

EV typically utilizes large electric motors that necessitate a significant quantity of batteries and sophisticated electronic power converters to supply the necessary high-level electrical power they require. The structure of multilevel inverters (MLIs) enables the synthesis of high-quality, high-voltage waveforms, making them ideal for high-power drive systems. In [9], the authors proposed the effectiveness of drive control using a MLI. The suggested method combines the use of sand cat swarm optimization and spiking neural networks. According to the findings, the suggested approach can outperform current methods based on torque ripple, energy efficiency, and speed tracking [10].

MLIs are capable of operating at both the fundamental switching frequency and a high rate of pulse-width modulation (PWM) switching [11]. It is well known that these inverters can produce low harmonic waveforms for high-voltage signals. However, adding more switching devices results in a system that becomes more complex and expensive, resulting in maintenance challenges [12]. Asymmetric MLIs are viewed as an effective solution for overcoming the limitations of traditional MLIs.

The goal of the paper is introduces a 21-asymmetric MLI with reduced switching for powering electric propulsion system of EV, with the proposed topology delivering notable enhancements in both performance and cost-efficiency compared to conventional asymmetric designs. The new aspect is that the article [13] addressed the 21-level inverter topology in an open loop and it used artificial neural networks for selective harmonic elimination PWM (SHE-ANN) modulation. This article is a continuation of the first, where we used the 21-level inverter within the electric EV's traction system (closed loop) using sinusoidal PWM (SPWM) modulation.

Subject of investigations. This paper presents a 21-hybrid asymmetric MLI reduced switching inverter within the EV's traction system for powering a PMSM with a nominal power of approximately 50 kW and a maximum torque of 255 N·m. Our traction system requires control laws that remain unaffected by disturbances, parameter changes, and nonlinearities. This study will employ a variable structure control approach, commonly referred to as SMC.

The proposed topology used to optimize the quality of the output voltage for improving the performance of the EV while minimizing the number of switching devices. It offers a cost-effective and simple system that is easy to maintain.

Electric propulsion system. Dynamics analysis. The propulsion system must produce enough traction effort at the wheel to counteract the combined forces of aerodynamic drag, rolling resistance, road inclination, and the force necessary to accelerate the vehicle. This section outlines the primary forces that enable a vehicle's operation. Figure 1 illustrates the main forces acting on the EV.

The force needed to drive the EV at the wheels is defined by the following equation [14, 15]:

$$\boldsymbol{F}_T = \boldsymbol{F}_{ro} + \boldsymbol{F}_{ad} + \boldsymbol{F}_{cr} + \boldsymbol{F}_{sf}\,, \tag{1}$$

where $\boldsymbol{F}_T$ is the traction force; $\boldsymbol{F}_{ro}$ is the force of rolling resistance; $\boldsymbol{F}_{ad}$ is the force of aerodynamic resistance; $\boldsymbol{F}_{cr}$ is the climbing resistance force; $\boldsymbol{F}_{sf}$ is the force of Stokes or viscous drag.

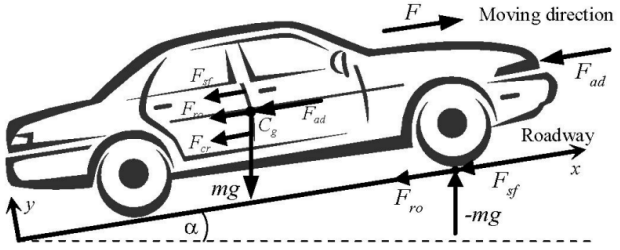

Fig. 1. Fundamental forces acting on an EV

The force of rolling resistance is:

$$\boldsymbol{F}_{ro} = C_d mg\cos\alpha\,. \tag{2}$$

The force that resists rolling $\boldsymbol{F}_{ro}$ is influenced by the vehicle's mass m acceleration due to gravity g, and the wheel's coefficient of rolling resistance C_d. In practice, with contemporary tires engineered for reduced tire resistance, a rolling resistance coefficient C_d is around 0.01 (and approximately 0.015 for conventional tires). The variation in this coefficient depends on the tire's width and the kind of road surface [16, 17].

The force of aerodynamic resistance

$$\boldsymbol{F}_{ad} = \frac{1}{2}PC_f A_f V_r^2 = \frac{1}{2}PC_f A_f\left(V + V_w\right)^2 \tag{3}$$

is proportional to the air density P, the square of the vehicle's speed $\boldsymbol{V}$, the wind speed $\boldsymbol{V}_w$, the vehicle's frontal surface area A_f, the relative speed of the vehicle V_r and its drag coefficient C_f, which varies between 0.25–0.5 depending on the shape of the vehicle body.

Climbing resistance force is:

$$\boldsymbol{F}_{cr} = \pm mg\sin\alpha\,, \tag{4}$$

where m is the vehicle mass, g is the gravitational acceleration constant; α is the grade angle.

The gravitational force acting on a vehicle driving on an inclined road depends on the road's slope. As shown in Fig. 1, this exerted force is positive while the automobile is climbing and negative while descending.

The force of Stokes or viscous drag is:

$$\boldsymbol{F}_{sf} = K_a V_r\,, \tag{5}$$

where K_a is the Stokes coefficient.

In [18] authors occasionally use the EV's acceleration force $\boldsymbol{F}_a$ in place of the viscous friction force $\boldsymbol{F}_{sf}$ as:

$$\boldsymbol{F}_a = m\lambda\frac{\mathrm{d}V_r}{\mathrm{d}t} = m + \sum J\left(\frac{i^2}{r}\right)\frac{\mathrm{d}V_r}{\mathrm{d}t}, \tag{6}$$

where λ is the mass factor, which varies with the engaged gear, ranges from 1.06 to 1.34; J is the moment of inertia at the circumference of the driving wheel; i is the gearbox ratio; r is the wheel radius.

The electric motor produces the traction force required for an EV to counteract the road resistance. Thus, the motion equation is expressed as:

$$K_m m\frac{\mathrm{d}V}{\mathrm{d}t} = \boldsymbol{F}_{tr} - \boldsymbol{F}_T\,, \tag{7}$$

where $\boldsymbol{F}_{tr}$ is the traction force of tires; K_m is the rotational inertia coefficient. The net force $\boldsymbol{F}_{tr} - \boldsymbol{F}_T$ accelerates the vehicle or decelerates it if $\boldsymbol{F}_T$ exceeds $\boldsymbol{F}_{tr}$.

The work A is given by the following expression:

$$A = \sum_{j=1}^{4} F_i \mathrm{d}x\,. \tag{8}$$

When the work is differentiated with respect to time, the resulting expression for mechanical power is:

$$P_{mech} = \frac{dA}{dt} = F\frac{dx}{dt} \Leftrightarrow P_{mech} = F \cdot V \,. \quad (9)$$

Description of the system. Figure 2 presents a diagram of the components of an EV powered by a system of electric traction. The main objective of the suggested design is to achieve speed control through SMC technique. The electric propulsion system comprises a DC voltage source, a 21-level reduced switching MLI, and a induction motor with a nominal power of approximately 50 kW and a maximum torque of 255 N·m.

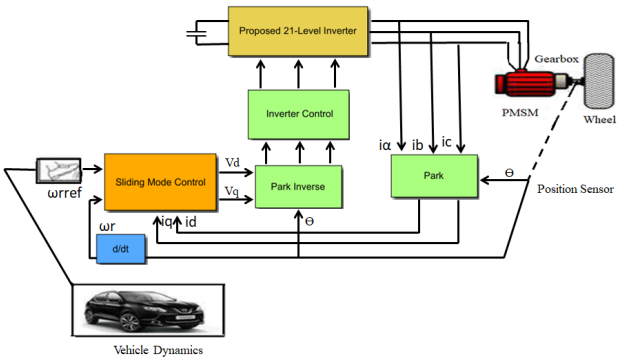

Fig. 2. The components of the traction system

The proposed 21-level inverter topology. Figure 3 shows the circuit model of the proposed 21-level inverter, designed with fewer switching devices. This inverter comprises 2 series-connected cells. The top cell consists of a basic H-bridge, constructed using switches $S_1 - S_4$, as well as 2 bidirectional switches, S_5 and S_6, along with 3-DC sources of equal voltage. The bidirectional switches S_5, S_6 manage the connection of the DC sources to produce the required staircase output voltage waveform. The lower cell contains an additional H-bridge, made up of switches $S_{p1} - S_{p4}$, which is connected to an isolated DC source [13].

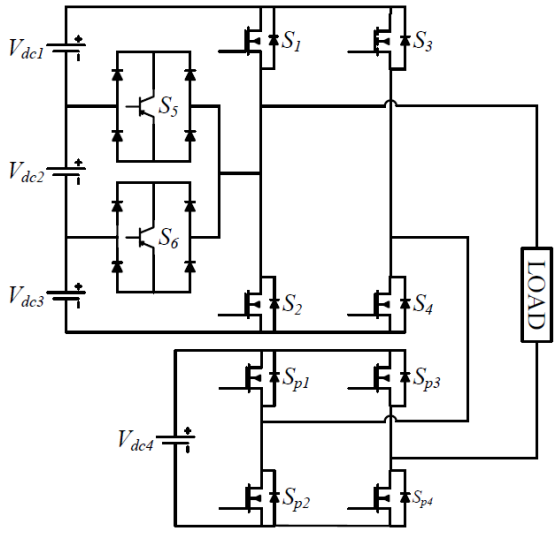

Fig. 3. The suggested 21-level inverter configuration [13]

Table 1 shows the allowed switching configurations for every possible combination. It is important to note that these combinations are only applicable under next conditions:

$$V_{dc1} = V_{dc2} = V_{dc3}\,; \quad (10)$$

$$V_{dc4} = 7 \cdot V_{dc1}\,. \quad (11)$$

Table 1

Output voltage levels (p.u.) with their respective conducting switches for the suggested 21-level inverter [13]

Voltage, p.u.	Switches in ON state	Voltage, p.u.	Switches in ON state
10	S_1, S_4, S_{p1}, S_{p4}	–10	S_3, S_2, S_{p2}, S_{p3}
9	S_4, S_5, S_{p1}, S_{p4}	–9	S_3, S_6, S_{p2}, S_{p3}
8	S_4, S_6, S_{p1}, S_{p4}	–8	S_5, S_3, S_{p2}, S_{p3}
7	S_2, S_4, S_{p1}, S_{p4}	–7	S_2, S_4, S_{p2}, S_{p3}
6	S_3, S_5, S_{p1}, S_{p4}	–6	S_6, S_4, S_{p2}, S_{p3}
5	S_3, S_6, S_{p1}, S_{p4}	–5	S_5, S_4, S_{p2}, S_{p3}
4	S_2, S_3, S_{p1}, S_{p4}	–4	S_1, S_4, S_{p2}, S_{p3}
3	S_1, S_4, S_{p2}, S_{p4}	–3	S_2, S_3, S_{p2}, S_{p4}
2	S_4, S_5, S_{p2}, S_{p4}	–2	S_3, S_6, S_{p2}, S_{p4}
1	S_4, S_6, S_{p2}, S_{p4}	–1	S_3, S_5, S_{p2}, S_{p4}
0	S_2, S_4, S_{p2}, S_{p4}	0	S_2, S_4, S_{p2}, S_{p4}

SMC strategy of the PMSM. The mathematical model of the PMSM in the stationary *d-q* coordinates system is [19, 20]:

$$\begin{cases} i_d = -\dfrac{R}{L_d} i_d + \dfrac{L_q}{L_d} p\omega_r i_q + \dfrac{1}{L_d} V_d; \\ i_q = -\dfrac{R}{L_d} i_q + \dfrac{L_d}{L_q} p\omega_r i_d - \dfrac{\varphi_f}{L_q} p\omega_r + \dfrac{1}{L_d} V_q; \\ \omega = \dfrac{3p}{2J}\left(\varphi_f i_q + \left(L_d - L_q\right) i_d i_q\right) - \dfrac{1}{J} C_r - \dfrac{f}{J}\omega_r, \end{cases} \quad (12)$$

where R is the stator resistance; L_d, L_q are the stator inductances; φ_f is the flux linkage of the permanent magnet; i_d, i_q are the stator currents; V_d, V_q are the stator voltages; ω_r is the mechanical speed; J is the inertia moment; f is the viscous friction coefficient, p is the poles pairs number; C_r is the load torque.

Our traction system requires control laws that remain unaffected by disturbances, parameter changes, and nonlinearities. This study will employ a variable structure control approach, commonly referred to as SMC.

The system represented by the state space equation given bellow is taken into consideration [21]:

$$[\dot{\boldsymbol{X}}] = \boldsymbol{A}[\boldsymbol{X}] + \boldsymbol{B}[\boldsymbol{U}], \quad (13)$$

where the state vector is represented by $[\boldsymbol{X}] \in R^n$, the control input vector by $[\boldsymbol{U}] \in R^n$, and the system parameter matrices by $[\boldsymbol{A}]$ and $[\boldsymbol{B}]$.

Selecting the quantity of switching surface $s(x)$ is the initial stage of the control design. This number typically equals the control vector's $[\boldsymbol{B}]$ dimension. To guarantee the variable x convergence to its reference x_{ref}, the authors [17] suggests the following general purpose for the switching surface:

$$S(x) = \left(\frac{d}{dt} + \lambda\right)^{n-1} e(x)\,, \quad (14)$$

where n is the relative degree; λ is the positive coefficient; and the vector of tracking errors is $e(x) = x_{ref} - x$.

The second step is to identify the control law that satisfies the requirements necessary for a sliding mode like to exist and be reachable [17]:

$$S(x) \cdot \dot{S}(x) < 0\,. \quad (15)$$

There are two parts to the control law:

$$\boldsymbol{U} = \boldsymbol{U}_{eq} + \boldsymbol{U}_n\,; \quad (16)$$

$$\boldsymbol{U_n} = K_x \text{sign}(S(x))\,, \quad (17)$$

where $\boldsymbol{U_n}$ is the correction factor; $\boldsymbol{U_{eq}}$ is the equivalent control vector; $\boldsymbol{U}$ is the control vector. $\boldsymbol{U_n}$ should be computed to satisfy the stability requirements for the selected control [17]; K_x is the constant.

In this study, the following sliding surfaces are selected as follows:

$$\begin{cases} S(i_d) = i_{d\,ref} - i_d; \\ S(i_q) = i_{q\,ref} - i_q; \\ S(\omega_r) = \omega_{r\,ref} - \omega_r. \end{cases} \quad (18)$$

The first order derivate of (18), gives:

$$\begin{cases} \dot{S}(i_d) = \dot{i}_{d\,ref} - \dot{i}_d; \\ \dot{S}(i_q) = \dot{i}_{q\,ref} - \dot{i}_q; \\ \dot{S}(\omega_r) = \dot{\omega}_{r\,ref} - \dot{\omega}_r. \end{cases} \quad (19)$$

The control vectors $\boldsymbol{V}_{deq}$, $\boldsymbol{V}_{qeq}$ and $\boldsymbol{i}_{deq}$ are obtained by imposing $\dot{S}(x) = 0$, consequently, the following relation provides the corresponding control components:

$$\begin{cases} \boldsymbol{V}_{deq} = L_d \dot{i}_{d\,ref} + R i_d - \omega_r L_q i_q; \\ \boldsymbol{V}_{qeq} = L_d \dot{i}_{q\,ref} + R i_q - \omega_r L_d i_d + \omega_r \varphi_f; \\ \boldsymbol{i}_{qeq} = \dfrac{J\dot{\omega}_{r\,ref} + pC_r + f\omega_r}{p((L_d - L_q) i_d + \sqrt{\dfrac{3}{2}}\varphi_f)}. \end{cases} \quad (20)$$

When substituting (17) and (20) into (16), the following control vector is applied in order to get good performances, dynamics, and commutations around the surfaces:

$$\begin{cases} \boldsymbol{V}_d = \boldsymbol{V}_{deq} + K_1 \text{sign}(S(i_d)); \\ \boldsymbol{V}_q = \boldsymbol{V}_{qeq} + K_2 \text{sign}(S(i_q)); \\ \boldsymbol{i}_q = \boldsymbol{i}_{qeq} + K_3 \text{sign}(S(\omega_r)), \end{cases} \quad (21)$$

where $K_1 - K_3$ are all positive constants.

Discussion of simulation results. Simulations were performed to characterize the vehicle traction system's behavior, using the model presented in Fig. 2. The simulations illustrate vehicle speed control with SMC technique driven by a novel 21-level inverter topology. The test cycle is the urban ECE-15 cycle (Fig. 4).

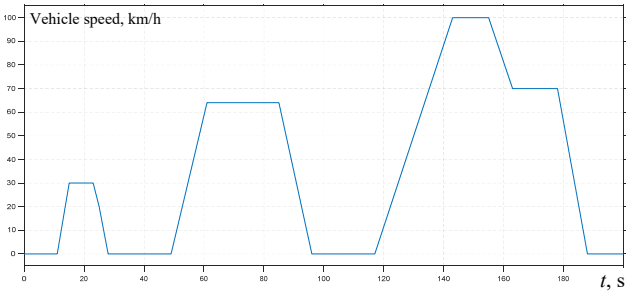

Fig. 4. European urban driving cycle ECE-15

To verify the suggested topology's effectiveness a comparative study has been done to demonstrate the merits of the proposed topology over of 2-level inverter topology. Total harmonic distortion (THD) was chosen as a quality index to evaluate the quality of the generated output voltage:

$$THD = \frac{\sqrt{\sum_{n=3}^{50} H_n^2 H_1}}{X} \cdot 100\% .$$

Figure 5,*a* shows the voltage wave forms generated by 2-level inverter topology. The spectra of the output voltage waveforms are shown in Fig. 5,*b*. THD is 73.39 %.

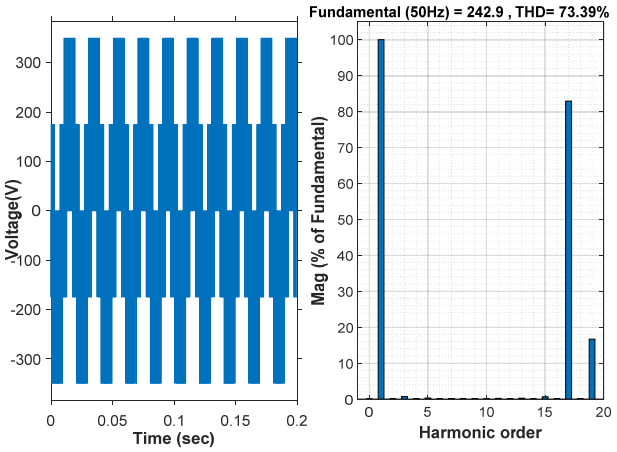

a *b*

Fig. 5. Voltage waveform produced by 2-level inverter along with its corresponding FFT analysis

Figure 6,*a* shows the voltage wave forms generated by a 21-level reduced switching inverter topology. The spectra of the output voltage waveforms are shown in Fig. 6,*b*. THD is 6.19 %.

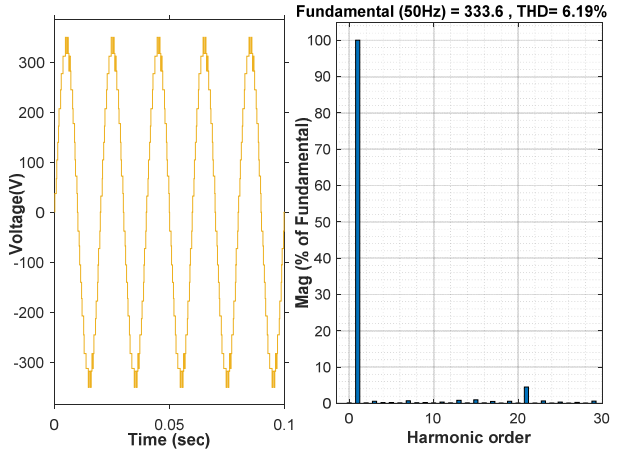

a *b*

Fig. 6. Voltage signal produced by the suggested 21-level inverter along with its corresponding FFT analysis

Reference tracking test. It is worth mentioning that the simulation was conducted using Europe's ECE-15 urban driving cycle. Within this cycle, 3 speed requests were applied in a trapezoidal form (30 rad/s, 65 rad/s, 100 rad/s). Additionally, a 10 % slope was applied between 16 and 23 s. This simulation's objective is to verify whether our method of control can be implemented in real-time and to track the behavior of the vehicle in the different modes under study.

Figures 7, 8 show the vehicle speed response in SMC technique. We observe that the rotation speed of the motor can rapidly track the reference rotation speed, a good tracking dynamics are observed. This command switches very quickly within its limits which impacts the overall command of the vehicle.

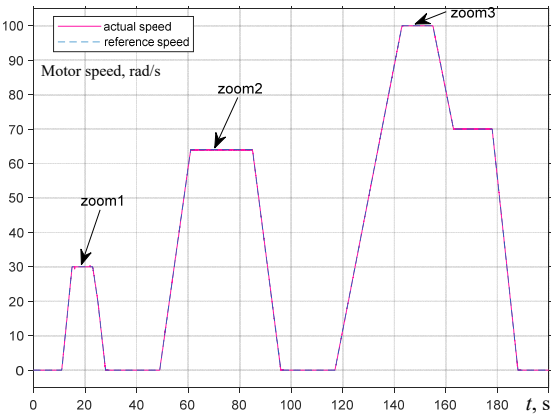

Fig. 7. The vehicle's motor rotation speed

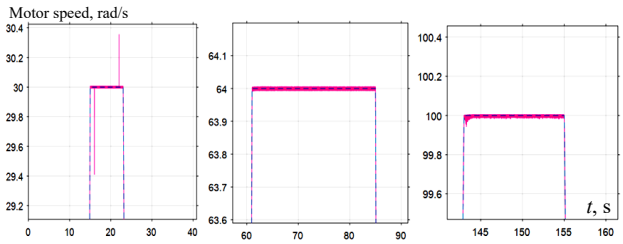

Fig. 8. Zoom of the reference and actual vehicle speed

Figure 9 shows the variation of electromagnetic torque as load torque changes. Figure 10 presents the results for the direct and quadrature currents. As outlined in the control strategy description, this method clearly maintains the direct current constant at zero, allowing only the quadrature component to respond to torque disturbances. This demonstrates the controller's excellent tracking capability ($i_{dref} = 0$). Furthermore, the i_q current and the electromagnetic torque exhibit identical profiles, confirming that decoupling has been successfully achieved.

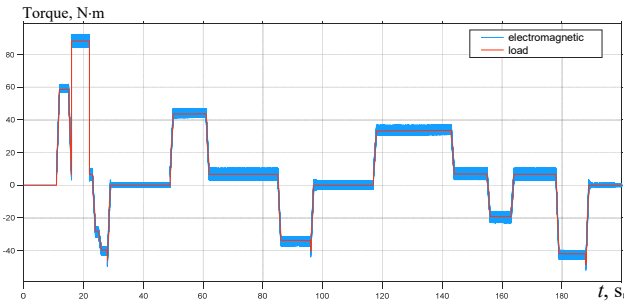

Fig. 9. Electromagnetic and load torques

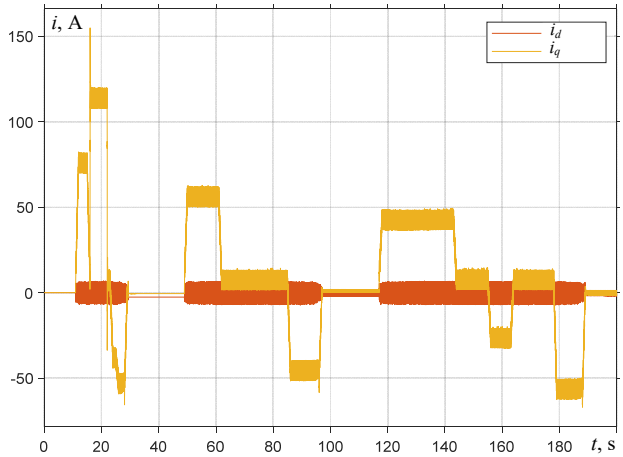

Fig. 10. Direct and quadratic currents

Conclusions. This paper aims to enhance EV performance by utilizing SMC technique for controlling a PMSM powered by a 21-level reduced switching inverter topology. The suggested SMC technique is reliable in situations where there are variations in the desired output due to fluctuations in the propulsion system's load.

Using MATLAB/Simulink proved that, using a 21-asymmetric MLI helps reduce harmonics contributing to optimize the quality of the output voltage, the THD was found to be 6.19 %, for improving the performance of the EV. The proposed topology delivering notable enhancements in both performance and cost-efficiency compared to conventional asymmetric designs. Future studies will propose a new control method that reduce chattering phenomenon of SMC method, to improve the performance of the controller system.

Conflict of interest. The authors declare that they have no conflicts of interest.

REFERENCES

1. Deng R., Xiang Y., Huo D., Liu Y., Huang Y., Huang C., Liu J. Exploring flexibility of electric vehicle aggregators as energy reserve. *Electric Power Systems Research*, 2020, vol. 184, art. no. 106305. doi: https://doi.org/10.1016/j.epsr.2020.106305.

2. Wang Y., John T., Xiong B. A two-level coordinated voltage control scheme of electric vehicle chargers in low-voltage distribution networks. *Electric Power Systems Research*, 2019, vol. 168, pp. 218-227. doi: https://doi.org/10.1016/j.epsr.2018.12.005.

3. Salehifar M., Moreno-Eguilaz M., Putrus G., Barras P. Simplified fault tolerant finite control set model predictive control of a five-phase inverter supplying BLDC motor in electric vehicle drive. *Electric Power Systems Research*, 2016, vol. 132, pp. 56-66. doi: https://doi.org/10.1016/j.epsr.2015.10.030.

4. Phan D., Bab-Hadiashar A., Fayyazi M., Hoseinnezhad R., Jazar R.N., Khayyam H. Interval Type 2 Fuzzy Logic Control for Energy Management of Hybrid Electric Autonomous Vehicles. *IEEE Transactions on Intelligent Vehicles*, 2021, vol. 6, no. 2, pp. 210-220. doi: https://doi.org/10.1109/TIV.2020.3011954.

5. Guezi A., Bendaikha A., Dendouga A. Direct torque control based on second order sliding mode controller for three-level inverter-fed permanent magnet synchronous motor: comparative study. *Electrical Engineering & Electromechanics*, 2022, no. 5, pp. 10-13. doi: https://doi.org/10.20998/2074-272X.2022.5.02.

6. Cai S., Kirtley J.L., Lee C.H.T. Critical Review of Direct-Drive Electrical Machine Systems for Electric and Hybrid Electric Vehicles. *IEEE Transactions on Energy Conversion*, 2022, vol. 37, no. 4, pp. 2657-2668. doi: https://doi.org/10.1109/TEC.2022.3197351.

7. Huang Z., Tang M., Golovanov D., Yang T., Herring S., Zanchetta P., Gerada C. Profiling the Eddy Current Losses Variations of High-Speed Permanent Magnet Machines in Plug-In Hybrid Electric Vehicles. *IEEE Transactions on Transportation Electrification*, 2022, vol. 8, no. 3, pp. 3451-3463. doi: https://doi.org/10.1109/TTE.2022.3152845.

8. Xu W., Junejo A.K., Liu Y., Hussien M.G., Zhu J. An Efficient Antidisturbance Sliding-Mode Speed Control Method for PMSM Drive Systems. *IEEE Transactions on Power Electronics*, 2021, vol. 36, no. 6, pp. 6879-6891. doi: https://doi.org/10.1109/TPEL.2020.3039474.

9. Chindamani M., Ravichandran C.S., Alamelumangai M. Drive Control using Multilevel Inverter for Electric Vehicle Application: A Hybrid SCSO-SNN Technique. *IETE Journal of Research*, 2024, vol. 70, no. 11, pp. 8232-8241. doi: https://doi.org/10.1080/03772063.2024.2378475.

10. Khemis A., Boutabba T., Drid S. Model reference adaptive system speed estimator based on type-1 and type-2 fuzzy logic sensorless control of electrical vehicle with electrical differential.

Electrical Engineering & Electromechanics, 2023, no. 4, pp. 19-25. doi: https://doi.org/10.20998/2074-272X.2023.4.03.
11. Djafer L., Taleb R., Toubal Maamar A.E., Mehedi F., Mostefaoui S.A., Rekmouche H. Analysis and Experimental Implementation of SHEPWM based on Newton-Raphson Algorithm on Three-Phase Inverter using Dspace 1104. *2023 2nd International Conference on Electronics, Energy and Measurement (IC2EM)*, 2023, pp. 1-6. doi: https://doi.org/10.1109/IC2EM59347.2023.10419389.
12. Djafer L., Taleb R., Mehedi F. Dspace implementation of real-time selective harmonics elimination technique using modified carrier on three phase inverter. *Electrical Engineering & Electromechanics*, 2024, no. 5, pp. 28-33. doi: https://doi.org/10.20998/2074-272X.2024.5.04.
13. Chabni F., Taleb R., Helaimi M. ANN-based SHEPWM using a harmony search on a new multilevel inverter topology. *Turkish Journal of Electrical Engineering & Computer Sciences*, 2017, vol. 25, no. 6, pp. 4867-4879. doi: https://doi.org/10.3906/elk-1703-122.
14. Li K., Ding J., Sun X., Tian X. Overview of Sliding Mode Control Technology for Permanent Magnet Synchronous Motor System. *IEEE Access*, 2024, vol. 12, pp. 71685-71704. doi: https://doi.org/10.1109/ACCESS.2024.3402983.
15. Araria R., Berkani A., Negadi K., Marignetti F., Boudiaf M. Performance Analysis of DC-DC Converter and DTC Based Fuzzy Logic Control for Power Management in Electric Vehicle Application. *Journal Européen Des Systèmes Automatisés*, 2020, vol. 53, no. 1, pp. 1-9. doi: https://doi.org/10.18280/jesa.530101.
16. Agrawal A., Singh R., Kumar N., Singh V.P., Alotaibi M.A., Malik H., Marquez F.P.G., Hossaini M.A. Mathematical Modeling of Driving Forces of an Electric Vehicle for Sustainable Operation. *IEEE Access*, 2023, vol. 11, pp. 95278-95294. doi: https://doi.org/10.1109/ACCESS.2023.3309728.
17. Al Halabi M., Al Tarabsheh A. Modelling of Electric Vehicles Using Matlab/Simulink. *SAE Technical Papers*, 2020, vol. 2020-January. doi: https://doi.org/10.4271/2020-01-5086.
18. Abul Masrur M. Hybrid and Electric Vehicle (HEV/EV) Technologies for Off-Road Applications. *Proceedings of the IEEE*, 2021, vol. 109, no. 6, pp. 1077-1093. doi: https://doi.org/10.1109/JPROC.2020.3045721.
19. Gao H., Zhang Z., Liu Y., Huang W., Xue H. Development and Analysis of Dual Three-Phase PMSM With Phase-Shifted Hybrid Winding for Aircraft Electric Propulsion Application. *IEEE Transactions on Transportation Electrification*, 2024, vol. 10, no. 3, pp. 6497-6508. doi: https://doi.org/10.1109/TTE.2023.3334026.
20. Hu S., Liang Z., Zhang W., He X. Research on the Integration of Hybrid Energy Storage System and Dual Three-Phase PMSM Drive in EV. *IEEE Transactions on Industrial Electronics*, 2018, vol. 65, no. 8, pp. 6602-6611. doi: https://doi.org/10.1109/TIE.2017.2752141.
21. Zhang C., He J., Jia L., Xu C., Xiao Y. Virtual line-shafting control for permanent magnet synchronous motor systems using sliding-mode observer. *IET Control Theory & Applications*, 2015, vol. 9, no. 3, pp. 456-464. doi: https://doi.org/10.1049/iet-cta.2014.0477.

Received 15.11.2024
Accepted 31.01.2025
Published 02.05.2025

L. Djafer[1], *PhD Student,*
R. Taleb[2], *Professor,*
F. Mehedi[3], *Associate Professor,*
A. Aissa Bokhtache[1], *Associate Professor,*
T. Bessaad[1], *Associate Professor,*
F. Chabni[4], *Associate Professor,*
H. Saidi[2], *Associate Professor,*
[1] Electrical Engineering Department,
Faculty of Technology, Hassiba Benbouali University of Chlef, Laboratoire Génie Electrique et Energies Renouvelables (LGEER), Chlef, Algeria,
e-mail: lem.djafer@gmail.com (Corresponding Author); a.aissabokhtache@gmail.com; ta.bessaad@gmail.com
[2] Laboratoire Génie Electrique et Energies Renouvelables (LGEER), Electrical Engineering Department,
Hassiba Benbouali University of Chlef, Algeria and Embedded Systems Research Unit of Chlef, Research Centre for Scientific and Technical Information (CERIST), Ben Aknoun, Algeria,
e-mail: r.taleb@univ-chlef.dz, hem.saidi@gmail.com
[3] Laboratoire Génie Electrique et Energies Renouvelables (LGEER), Faculty of Technology,
Hassiba Benbouali University of Chlef, Algeria,
e-mail: f.mehedi@univ-chlef.dz
[4] Electronics Department, Abdellah Morseli University Center of Tipaza, Laboratoire Génie Electrique et Energies Renouvelables (LGEER) of Chlef, Tipaza, Algeria,
e-mail: fayssalc@gmail.com

How to cite this article:
Djafer L., Taleb R., Mehedi F., Aissa Bokhtache A., Bessaad T., Chabni F., Saidi H. Electric drive vehicle based on sliding mode control technique using a 21-level asymmetrical inverter under different operating conditions. *Electrical Engineering & Electromechanics*, 2025, no. 3, pp. 31-36. doi: https://doi.org/10.20998/2074-272X.2025.3.05